Advanced Composite Materials
Publication details, including instructions for authors and subscription information:
http://www.tandfonline.com/loi/tacm20

On the specimen for interfacial fracture toughness evaluation of foam-core sandwich structures

Tomohiro Yokozeki [a]

[a] Department of Aeronautics and Astronautics, The University of Tokyo, 7-3-1 Hongo, Bunkyo-ku, Tokyo, 113-8656, Japan

Version of record first published: 12 Nov 2012.

To cite this article: Tomohiro Yokozeki (2012): On the specimen for interfacial fracture toughness evaluation of foam-core sandwich structures, Advanced Composite Materials, 21:5-6, 491-503

To link to this article: http://dx.doi.org/10.1080/09243046.2012.743717

Advanced Composite Materials
Vol. 21, Nos. 5–6, October–December 2012, 491–503

On the specimen for interfacial fracture toughness evaluation of foam-core sandwich structures

Tomohiro Yokozeki*

Department of Aeronautics and Astronautics, The University of Tokyo, 7-3-1 Hongo, Bunkyo-ku, Tokyo 113-8656, Japan

(*Received 27 July 2012; accepted 24 September 2012*)

Foam-core sandwich specimens for interfacial fracture toughness measurement are designed based on the prediction method of steady-state crack location in foam-core sandwich beams using the crack deflection model developed previously. This paper derives the necessary condition that the face sheet debonding grows along the interface between the face sheet and the core during the fracture toughness tests. The recommended specimen thickness ratios for several testing methods are presented. Finally, the physical meaning of the derived condition is explained, and the effect of residual thermal stresses on the condition is discussed.

Keywords: foam-core sandwich; fracture toughness test; debonding; specimen design; crack kinking

1. Introduction

Sandwich structures are attractive structural materials for use in aerospace structures because of their high performance (e.g. bending stiffness). The application ratio of sandwich structures to aircraft [1], maritime, and civil structures reveals a tendency toward their dramatically increased use. However, sandwich structures are vulnerable to face sheet debonding, core cracking, and delaminations inside the face sheet [2–4], which limits their application in large transport aircraft to secondary structures such as fairings, ailerons, or cabin linings. Crack-stopper elements are under development to prevent the face sheet debonding [5–7]. Debonding between the face sheet and the core needs to be well characterized for attaining a comprehensive understanding of the damage tolerance behavior of sandwich structures.

To characterize the face/core debonding fracture toughness of sandwich strcutures, double cantilever beam (DCB) [8,9], single cantilever beam (SCB) [10,11], tilted sandwich debond (TSD) [12,13], and mixed mode bending (MMB) [14] tests have been proposed (see Figure 1). The SCB tests or TSD tests are recommended as a standard test in Ref. [11]. In order to develop the standard test method, it is necessary to investigate effects of the specimen geometry, testing procedure, etc. and to define the recommended method in the case of sandwich beam specimens.

During fracture toughness tests of foam core sandwich beams, the possibility exists that the crack propagates in a plane that is different from the original crack plane [9], as shown in

*Email: yokozeki@aastr.t.u-tokyo.ac.jp

ISSN 0924-3046 print/ISSN 1568-5519 online

http://dx.doi.org/10.1080/09243046.2012.743717
http://www.tandfonline.com

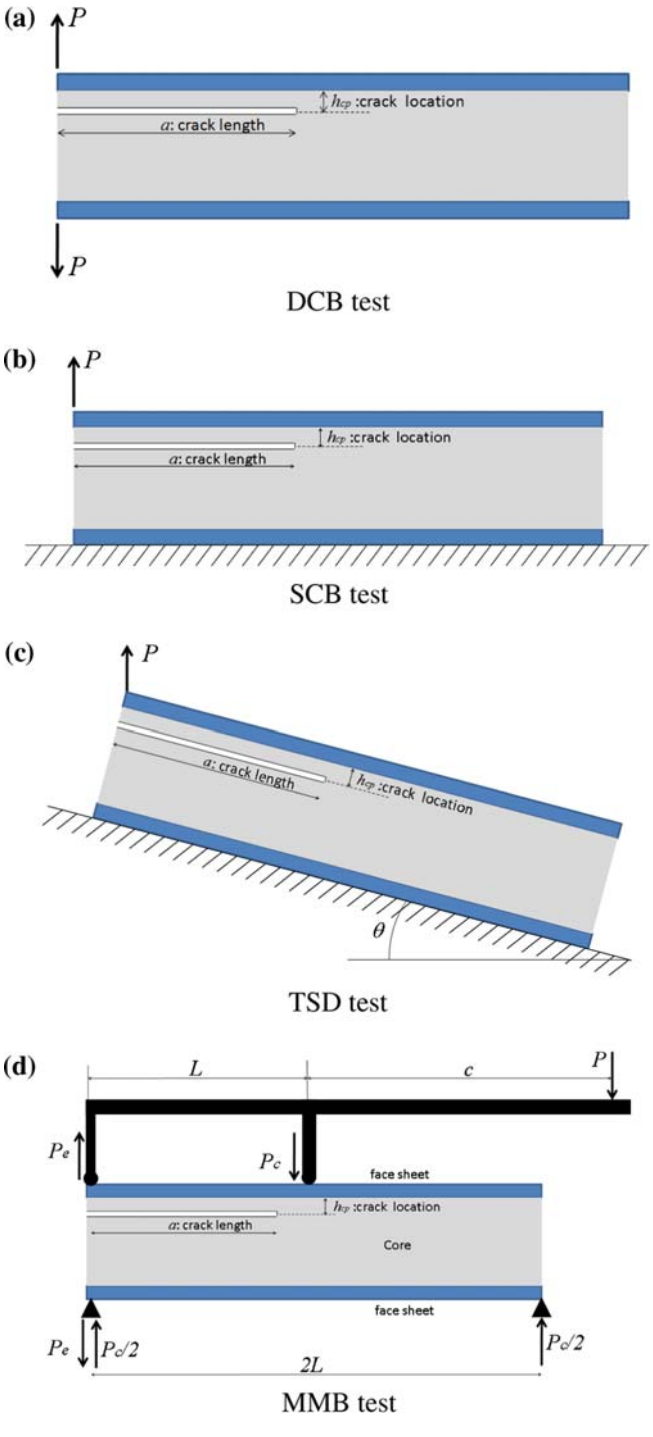

Figure 1. Test methods for fracture toughness evaluation of sandwich structures: (a) DCB test, (b) SCB test, (c) TSD test, and (d) MMB test.

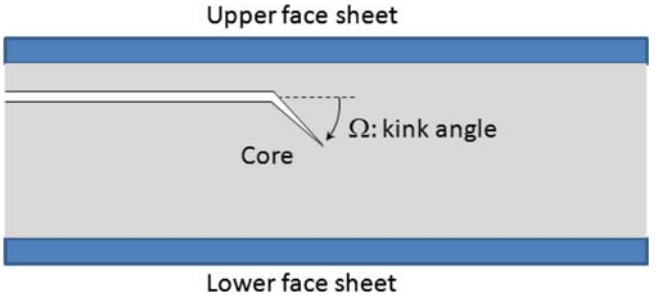

Figure 2. Crack kinking in foam core sandwich structures.

Figure 2. For example, the initial crack plane is set along the interface between a face sheet and a core, but the crack might grow obliquely into the core or the face sheet when a load is applied. The sandwich specimens often suffer from this crack kinking during the fracture toughness tests. As the crack kinking behavior depends on the used materials, specimen geometry, and loading conditions [15,16], it is useful if the specimen geometry, that is suitable for interfacial fracture toughness evaluation, is known prior to the tests. It might be necessary to consider the testing method based on the prevention of face sheet failure during loading, the effect of large deformation, how to calculate fracture toughness, and the effect of compliance of the fixtures. In this study, we focus on the crack kinking behavior in foam core sandwich beams, and derive the sizing of appropriate specimen geometry for interfacial fracture toughness evaluation using the previous analytical model [15,16].

In the present paper, we explain the predictive method of steady-state crack location during the fracture toughness tests of foam core sandwich specimens using the previous model [16] with the comparison to available experimental results. Then, we derive the necessity condition that the face sheet debonding grows along the interface between the face sheet and the core during the fracture toughness tests. The recommended specimen geometry is shown for several testing methods. Finally, the derived necessity conditions are discussed based on the physical meanings. The effect of thermal stresses in sandwich specimens (in the case that cured temperature is different from the operation temperature) on the necessary conditions is also investigated.

2. Crack kinking model

2.1. Derivation of crack tip forces using a bi-layer beam model

Consider a sandwich beam with a crack as presented in Figure 3(a). Two sublaminates are defined and the crack plane is regarded as the interface between the two sublaminates, see Figure 3(b). Subscripts 1 and 2 denote the upper sublaminate and the lower sublaminate, respectively. Each sublaminate is modeled as a Timoshenko beam. The local coordinates (x_i and z_i) and the global coordinates (x) are defined in the manner presented in Figure 3(b), where the origins of the local coordinates are located in the middle plane of each sublaminate. Displacements in each sublaminate (U, W) of the bi-layer model, as presented in Figure 3(b), are assumed to be expressed in terms of those at the middle surface of each sublaminate (u, ϕ, w) in the following way.

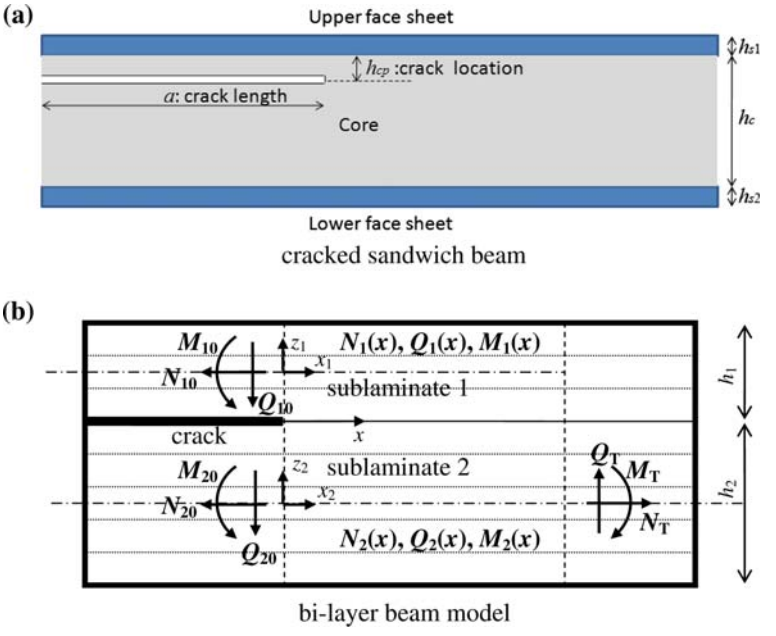

Figure 3. Analytical bi-layer beam model for a cracked sandwich beam: (a) cracked sandwich beam and (b) bi-layer beam model.

$$\begin{aligned} U_i(x_i, z_i) &= u_i(x) + z_i\phi_i(x) \\ W_i(x_i, z_i) &= w_i(x) \end{aligned} \tag{1}$$

where, subscript i denotes each sublaminate. The constitutive equations of each sublaminate including initial strains are described as

$$\begin{aligned} \left\{ \begin{matrix} N_i \\ M_i \end{matrix} \right\} &= \begin{bmatrix} A_i & B_i \\ B_i & D_i \end{bmatrix} \left\{ \begin{matrix} \varepsilon_i \\ \kappa_i \end{matrix} \right\} - \left\{ \begin{matrix} N_{Ti} \\ M_{Ti} \end{matrix} \right\}, \\ Q_i &= \kappa C_i \gamma_i \end{aligned} \tag{2}$$

where, N, M, and Q are the cross-sectional resultant extensional force, moment, and the shear force, respectively. The first equation of Equation (2) can be expressed alternatively as

$$\left\{ \begin{matrix} \varepsilon_i \\ \kappa_i \end{matrix} \right\} = \begin{bmatrix} a_i & b_i \\ b_i & d_i \end{bmatrix} \left\{ \begin{matrix} N_i \\ M_i \end{matrix} \right\} + \left\{ \begin{matrix} \alpha_{Ni} \\ \alpha_{Mi} \end{matrix} \right\}. \tag{3}$$

In these equations, the following relations hold.

$$\varepsilon_i = \frac{\mathrm{d}u_i}{\mathrm{d}x}, \quad \kappa_i = \frac{\mathrm{d}\phi_i}{\mathrm{d}x}, \quad \gamma_i = \phi_i + \frac{\mathrm{d}w_i}{\mathrm{d}x} \tag{4}$$

$$\begin{aligned} A_i = B\int E_i dz_i, \quad B_i = B\int E_i z_i dz_i, \quad D_i = B\int E_i z_i^2 dz_i, \quad C_i = B\int G_i dz_i \\ N_{Ti} = B\int E_i \alpha_i \Delta T dz_i, \quad M_{Ti} = B\int E_i \alpha_i \Delta T z_i dz_i \end{aligned} \tag{5}$$

$$a_i = \frac{D_i}{A_i D_i - B_i^2},\ b_i = \frac{-B_i}{A_i D_i - B_i^2},\ d_i = \frac{A_i}{A_i D_i - B_i^2}$$
$$\alpha_{Ni} = \frac{D_i N_{Ti} - B_i M_{Ti}}{A_i D_i - B_i^2},\ \alpha_{Mi} = \frac{A_i M_{Ti} - B_i N_{Ti}}{A_i D_i - B_i^2} \tag{6}$$

In these equations, B denotes the beam width, E represents the in-plane Young's modulus, G signifies the out-of-plane shear modulus, κ is the shear factor (5/6 is used for the rectangular cross section in this study), α stands for thermal expansion coefficient, and ΔT is the difference between the operating temperature and the stress-free temperature.

By considering the equilibrium equations and the displacement continuity in the intact regions, the stress distributions in the sublaminates can be derived [15,16]. At the crack tip, concentric shear and normal forces are expected to exist in this bi-layer shear-deformable model, as presented in Figure 4, and the crack tip forces (N_c and Q_c) can be expressed by considering the force balance as

$$N_c = \frac{2(M\xi - N\eta)}{h_1\xi + 2\eta}$$
$$Q_c = -Q - \lambda\left(M + \tfrac{h_1}{2}N\right) \tag{7}$$

where,

$$N = N_{10} - N_{1P},\quad Q = Q_{10} - Q_{1P},\quad M = M_{10} - M_{1P} \tag{8}$$

$$\eta = a_1 + a_2 - \tfrac{h_1}{2}b_1 + \left(\frac{h_1}{2} + h_2\right)b_2 + \frac{h_2(h_1 + h_2)}{4}d_2$$
$$\xi = -b_1 - b_2 + \frac{h_1}{2}d_1 - \frac{h_2}{2}d_2 \tag{9}$$

hold. The parameters of Equation (8) (e.g. N_{10}, N_{1P}) are given by overall loading conditions, material properties, and geometries of the face sheet and the core, as discussed in Section 3. The energy release rates associated with the crack growth can be expressed in terms of crack tip forces [15,16] as

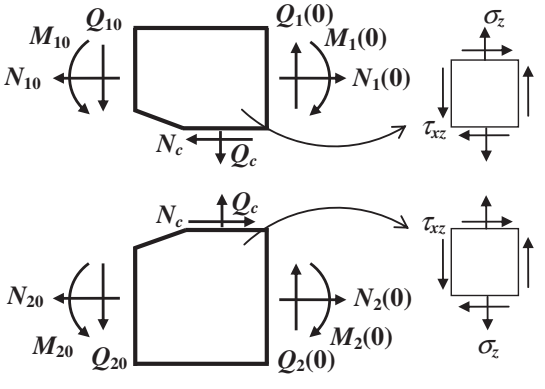

Figure 4. Crack tip forces.

$$G_{\mathrm{I}} = \frac{1}{2B}\left(\frac{1}{\kappa C_1} + \frac{1}{\kappa C_2}\right) Q_c^2$$
$$G_{\mathrm{II}} = \frac{1}{2B}\left(\eta + \frac{h_1}{2}\xi\right) N_c^2 \tag{10}$$

2.2. Prediction of crack kinking angle

In the case of fracture toughness tests of foam core sandwich beams, the possibility exists that the crack propagates in a plane with the angle of Ω from the original crack plane as shown in Figure 2. The energy release rates derived in the previous section are utilized to predict the crack kinking angle, Ω, in the following way. It is noted that it is necessary to analyze the oscillatory stress fields in the case of dissimilar interface crack problem. In the present study, the foam core is regarded as a homogeneous isotropic material, and it is assumed that the present analysis is valid when the crack location, h_{cp}, holds $0 \leq h_{\mathrm{cp}} \leq h_c$ (h_c is the core thickness).

Stress intensity factors can be determined from the energy release rates using the equation below.

$$K_{\mathrm{I}} = \begin{cases} \sqrt{E_c G_{\mathrm{I}}} & (Q_c > 0) \\ -\sqrt{E_c G_{\mathrm{I}}} & (Q_c < 0) \end{cases}$$
$$K_{\mathrm{II}} = \begin{cases} \sqrt{E_c G_{\mathrm{II}}} & (N_c > 0) \\ -\sqrt{E_c G_{\mathrm{II}}} & (N_c < 0) \end{cases} \tag{11}$$

Therein, E_c denotes the Young's modulus of the foam core. Signs of the stress intensity factors can be determined using Equation (11) considering the signs of crack tip forces corresponding to the stress definition. The negative value of K_I indicates the unrealistic penetration of crack surfaces, but K_{I} should be always positive without penetration.

Erdogan and Sih [17] demonstrated experimentally that cracks in homogeneous isotropic materials tend to propagate in the plane free from shear stresses. This condition results in the determination of the crack kink angle, Ω, as presented below.

$$\Omega = 2\tan^{-1}\left[\frac{\sqrt{1 + 8\left(\frac{K_{\mathrm{II}}}{K_{\mathrm{I}}}\right)^2} - 1}{4\left(\frac{K_{\mathrm{II}}}{K_{\mathrm{I}}}\right)}\right] \tag{12}$$

In the present study, Equation (12) is used for the crack kinking angle of a cracked foam core sandwich beam when the crack location is h_{cp} from the upper interface between the face sheet and the core. It should be noted that signs of crack kinking angle coincide with signs of crack tip force N_c (see Equation (11)), because K_{I} is always positive.

2.3. Steady-state crack location

In the previous study [16], the predictive method of crack kinking angle shown in the previous section was verified by comparing the predictions with the available experimental data of foam core sandwich beams by Carlsson et al. [9]. If we plot the predicted crack kinking angles as a function of crack location, h_{cp}, the steady-state crack location can be predicted.

For example, crack kinking angles are predicted as a function of crack location in the cases of I41 and I50 specimens in Ref. [9] as shown in Figure 5. Specimen I40 has the core

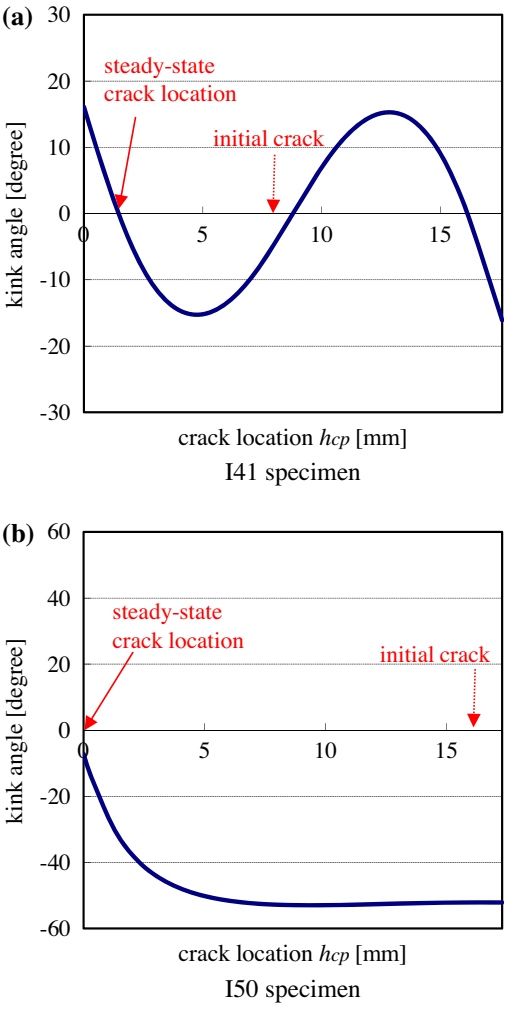

Figure 5. Predicted crack kink angle as a function of crack location: (a) I41 specimen and (b) I50 specimen.

thickness of 17.6 mm, and initial crack location, h_{cp}, is 8.1 mm. In this case, the predicted crack kinking angle is negative, see Figure 5. Therefore, it is expected that the crack kinks upwards. When the crack plane moves upwards (i.e. when the crack location, h_{cp}, decreases), the predicted crack kinking angle remains negative. This means that the crack would continue to kink upwards. However, when the crack location, h_{cp}, is lower than about 1.5 mm, the predicted crack kinking angle becomes positive. The crack tends to kink upwards when h_{cp} is larger than 1.5 mm and kink downwards when h_{cp} is lower than 1.5 mm. Therefore, it is expected that the steady-state crack location is 1.5 mm in I41 specimen. In a similar way, I50 specimen in Ref. [9] is discussed. Specimen I50 has the core thickness of 17.3 mm, and initial crack location, h_{cp}, is 16.9 mm. The predicted crack kinking angles are negative irrespective of crack location. This means that the crack kinks upwards to the upper interface. The face sheet is fiber-reinforced plastic (FRP). There is neither failure in the FRP face sheet nor crack penetration into face sheet. Therefore, the crack stably grows at the interface between the upper face sheet and the core in I50 specimen.

Table 1. Comparison of the predicted steady-state crack location with the experimental data in Ref. [9].

Specimen	Core thickness (mm)	Initial crack location (mm)	Final crack location (mm)	Predicted steady-state crack location (mm)
I30	14.2	7.6	7.0–7.5	7.1
I40	15.6	0.7	2.0–3.0	2.5
I41	17.6	8.1	1.5–2.5	1.5
I43	17.2	8.9	0–0.5	0
I45	17.6	1.2	8.0–9.0	8.3
I50	17.3	16.9	0–0.5	0
T1	37.9	0.8	0–0.5	0

The predicted steady-state crack locations are compared with the available experimental data in Ref. [9] as shown in Table 1. Fairly good agreement between the predictions and experimental results is obtained. It is confirmed that steady-state crack location including the interfaces between the face sheets and the core can be predicted using the present analysis.

3. Sizing of sandwich specimen for interfacial fracture toughness characterization

3.1. Necessary conditions for steady-state interfacial crack growth

In the previous section, it was demonstrated that steady-state crack location in the foam core including the interfaces between the face sheets and the core can be predicted using the crack kinking analysis. In order to evaluate the fracture toughness associated with interfacial crack growth between the face sheet and the core, it is necessary to prepare sandwich beam specimens in which the crack grows stably along the interface. In this section, necessary conditions for steady-state interfacial crack growth are derived.

Consider a sandwich specimen with a pre-crack along the interface between the upper face sheet and the core. When we neglect the crack penetration into the face sheet, it is considered that negative or zero crack kinking angle in the case of $h_{\mathrm{cp}}=0$ is the necessary condition for crack growth along the upper interface. Note that crack deflection or jump into the core or face sheet might be possible depending on the stress fields and the combination of material properties of constituent materials (e.g. fracture toughness and strength). Such phenomena are not considered herein.

Based on Equation (12), negative or zero crack kinking angle indicates negative or zero $K_{\mathrm{II}}/K_{\mathrm{I}}$. As the K_{I} is always positive, this condition means negative or zero K_{II}. In addition, it is derived that negative or zero crack tip force, N_c, is the necessary condition for steady-state interfacial crack growth when $h_{\mathrm{cp}}=0$. Using Equation (7), this condition is rewritten by

$$M\xi - N\eta \leq 0 \tag{13}$$

as the denominator of the right-hand side of Equation (7) is positive.

3.2. DCB specimen

Consider a DCB specimen with the crack length of a and the applied shear load of P. In this case, the parameters in Equation (8) are expressed as [15]

$$N_{10}=0,\ Q_{10}=-P,\ M_{10}=-Pa \tag{14}$$

$$N_{1p} = \frac{(d_1+d_2)(\alpha_{N2}-\alpha_{N1}) + \left(b_1+b_2+\frac{h_1+h_2}{2}d_2\right)\alpha_{M1} + \left(-b_1-b_2+\frac{h_1+h_2}{2}d_1\right)\alpha_{M2}}{(d_1+d_2)\eta + \left(b_1+b_2+\frac{h_1+h_2}{2}d_2\right)\xi}$$
$$M_{1p} = \frac{1}{\xi}\{\eta N_{1P} + (\alpha_{N1}-\alpha_{N2}) - \tfrac{h_1}{2}\alpha_{M1} - \tfrac{h_2}{2}\alpha_{M2}\} \tag{15}$$
$$Q_{1p} = 0$$

As a special case, we neglect the initial thermal strains. In addition, it is assumed that the face sheets and the core are homogeneous materials (Young's moduli are denoted as E_f and E_c, and the thicknesses are h_f and h_c for face sheet and the core, respectively), and the upper face sheet and the lower face sheet have the identical material properties and thickness. In this case, Equation (13) is expressed as $\xi \geq 0$, and the following condition is derived.

$$(2\alpha^2-\alpha)\bar{h}^3 - 5\alpha\bar{h}^2 - 4\alpha\bar{h} - 1 \geq 0 \tag{16}$$

$$\alpha = \frac{E_f}{E_c}, \quad \bar{h} = \frac{h_f}{h_c} \tag{17}$$

The above condition is plotted in Figure 6. The horizontal axis is α ($=E_f/E_c$) and the vertical axis is $\bar{h}$ ($=h_f/h_c$). The region below the solid line indicates the condition satisfying Equation (16). Specimen dimension (i.e. maximum thickness ratio, h_f/h_c) is prescribed by the modulus ratio (E_f/E_c). Specifically, in the case of sandwich beams with carbon fiber-reinforced plastic (CFRP) or glass fiber-reinforced plastic (GFRP) face sheets and typical foam core (i.e. $\frac{E_c}{E_f} \leq 0.01$), the following approximated equation is obtained.

$$\left(\frac{h_f}{h_c}\right)_{\max} \approx 1.5\sqrt{\frac{E_c}{E_f}} \qquad \left(\frac{E_c}{E_f} \leq 0.01\right) \tag{18}$$

When DCB tests are used for the evaluation of interfacial fracture toughness associated with debonding between the face sheet and the core, the author recommends the specimen

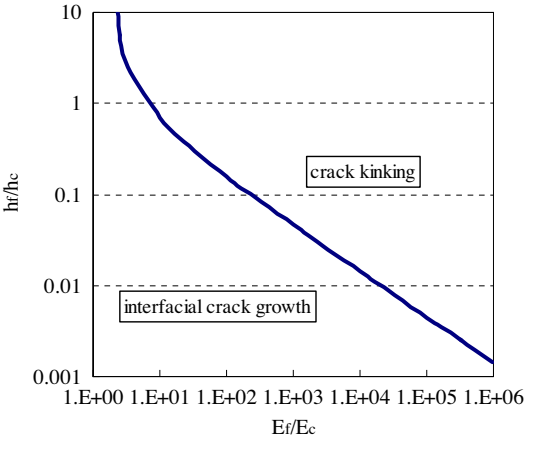

Figure 6. Sizing map of DCB specimen.

dimension satisfying Equation (16) (i.e. Figure 6) or Equation (18). Note that these conditions are valid when the upper face sheet and the lower face sheet are identical.

3.3. SCB specimen

In the case of SCB tests, the lower face sheet is rigid or completely fixed to the rigid fixture. Thus, the stiffness of the lower sublaminate is infinity (i.e. the compliance is zero; $a_2 = b_2 = d_2 = 0$). The loading condition is same as DCB tests. When we neglect initial thermal strains and assume that the upper face sheet is homogeneous (i.e. $b_1 = 0$), Equation (13) is rewritten by

$$\xi = \frac{h_1}{2} d_1 \geq 0 \tag{19}$$

This condition is always satisfied. Therefore, in the case of SCB tests, the crack stably grows along the upper interface independently of specimen dimensions. It should be noted that TSD test is the inclined version of SCB test, and the necessary condition is always satisfied, too.

It can be concluded that crack kinking is not induced in SCB tests and TSD tests of sandwich beam specimens, and thus, specimen configurations are not restricted in terms of crack kinking problem. The readers should refer to Refs. [10,11] on the specimen sizing of SCB specimens considering the conditions to prevent the face sheet failure, the effect of large deflection during loading, etc.

3.4. MMB specimen

The testing apparatus of MMB specimen is shown in Figure 1(d). The loading conditions give

$$P_e = P\frac{c}{L},\ P_c = P\frac{c+L}{L} \tag{20}$$

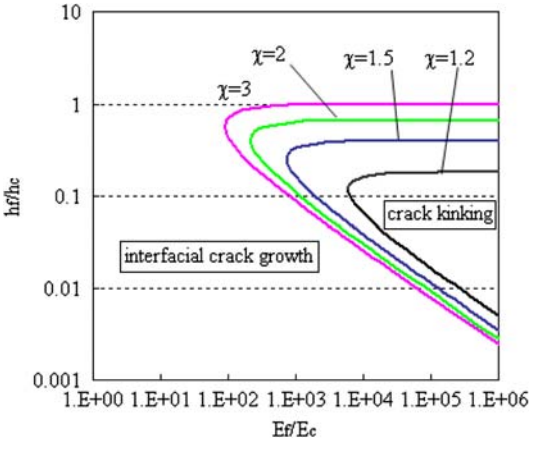

Figure 7. Sizing map of MMB specimen.

and the parameters in Equation (8) are expressed as [15]

$$N_{10} = 0, \quad Q_{10} = -P_e, \quad M_{10} = -P_e a \tag{21}$$

$$\begin{aligned} N_{1p} &= -\frac{\left(b_2 d_1 - b_1 d_2 + \frac{h_1+h_2}{2} d_1 d_2\right)}{(d_1+d_2)\eta + \left(b_1 + b_2 + \frac{h_1+h_2}{2} d_2\right)\xi} \frac{P_c}{2} a \\ &+ \frac{(d_1+d_2)(\alpha_{N2} - \alpha_{N1}) + \left(b_1 + b_2 + \frac{h_1+h_2}{2} d_2\right)\alpha_{M1} + \left(-b_1 - b_2 + \frac{h_1+h_2}{2} d_1\right)\alpha_{M2}}{(d_1+d_2)\eta + \left(b_1 + b_2 + \frac{h_1+h_2}{2} d_2\right)\xi} \\ M_{1p} &= \frac{1}{\xi}\left\{\eta N_{1P} + \left(b_2 + \frac{h_2}{2} d_2\right)\frac{P_c}{2} a + (\alpha_{N1} - \alpha_{N2}) - \frac{h_1}{2}\alpha_{M1} - \frac{h_2}{2}\alpha_{M2}\right\} \\ Q_{1p} &= -\frac{P_c}{2}\left\{\left(\frac{\eta}{\xi} + \frac{h_1}{2}\right)\frac{d_2\xi + (d_1+d_2)\left(b_2 + \frac{h_2}{2} d_2\right)}{(d_1+d_2)\eta + \left(b_1 + b_2 + \frac{h_1+h_2}{2} d_2\right)\xi} - \frac{b_2 + \frac{h_2}{2} d_2}{\xi}\right\} \end{aligned} \tag{22}$$

When we neglect the initial thermal strains and assume that the face sheets and the core are homogeneous materials, and the upper and lower face sheets have identical thickness, Equation (13) is expressed by

$$(1+\chi)\alpha^2 \bar{h}^4 + \{8\chi\alpha + 2(1-\chi)\alpha^2\}\bar{h}^3 + \alpha(1+11\chi)\bar{h}^2 + 8\chi\alpha\bar{h} + 2\chi \geq 0 \tag{23}$$

where, $\chi = c/L$ holds.

This condition is plotted with variation of χ in Figure 7. Decrease in χ results in lower possibility of crack kinking (i.e. crack growth along the interface is more susceptible). Compared to DCB specimens, the restrictive condition of specimen dimensions (i.e. h_f/h_c) is mitigated. It is concluded that crack growth along the interface is achieved during the MMB test in the case of specimens satisfying the dimensional condition of DCB specimens.

4. Discussion

4.1. On the necessary conditions for steady-state interfacial crack growth

This section gives another insight of the derived condition for steady-state interfacial crack growth. For example, in the case of DCB specimen with a crack at the interface between the upper face sheet and the core, the necessary condition is expressed by Equation (16). This condition is identical to the condition of $\xi \geq 0$.

In-plane normal strain ($\varepsilon^{(u)}$) at the crack tip ($x_1 = 0$, $z_1 = -h_f/2$) in the upper face sheet is derived as the following equation by using Equations (1), (3), and (4), when we set $M_1 = -Pa$

$$\varepsilon^{(u)} = \frac{\mathrm{d}U_1}{\mathrm{d}x}\left(0, -\frac{h_f}{2}\right) = \frac{h_f}{2} d_1 \times Pa \tag{24}$$

Note that the face sheet is assumed as homogeneous material (i.e. $b_1 = 0$). In a similar way, in-plane normal strain ($\varepsilon^{(l)}$) at the crack tip ($x_2 = 0$, $z_2 = (h_c + h_f)/2$) in the lower sublaminate is expressed as

$$\varepsilon^{(l)} = \frac{\mathrm{d}U_2}{\mathrm{d}x}\left(0, \frac{h_f + h_c}{2}\right) = \left(b_2 + \frac{h_f + h_c}{2} d_2\right) \times Pa \tag{25}$$

Therefore, ξ is expressed as

$$\xi = -b_2 + \frac{h_f}{2} d_1 - \frac{h_f + h_c}{2} d_2 = \frac{\left(\varepsilon^{(u)} - \varepsilon^{(l)}\right)}{Pa} \tag{26}$$

Equation (26) indicates that ξ is related to the strain difference between the upper surface and the lower surface at the crack tip. When the normal strain at the upper surface is equal to or larger than that at the lower surface, the crack grows along the interface. From Figure 4, the condition that the upper strain is equal to or larger than the lower strain means that the crack tip force N_c is zero or negative. Thus, steady-state interfacial crack growth condition is directly related to strain difference between the upper and lower surfaces.

It should be noted that the derived conditions for steady-state interfacial crack growth coincide with the above-mentioned strain difference condition not only in DCB test but other tests.

4.2. Effects of thermal strain

Laminated structures including sandwich structures suffer from residual thermal stresses owing to the difference between the curing temperature and the operating temperature. The residual thermal stresses or residual thermal deformation influences energy release rates or crack tip forces. Therefore, the residual thermal stresses have effects on the condition of steady-state interfacial crack growth.

As an example, consider a DCB sandwich specimen consisting of homogeneous upper and lower face sheets with identical material and thickness. Consideration of residual thermal stresses in Equation (13) results in

$$M\xi - N\eta = -Pa\xi + (\alpha_{N2} - \alpha_{N1}) + \frac{h_f + h_c}{2}\alpha_{M2} \leq 0 \tag{27}$$

Note that this value represents the strain difference described in Section 4.1. In typical sandwich structures, thermal expansion coefficient of the core is higher than that of face sheet, resulting in the fact that the underlined portion in Equation (27) is negative. The condition of Equation (27) is mitigated compared to the condition of $\xi \geq 0$ in the case of a DCB specimen without residual thermal stresses.

When the residual thermal stresses are induced in a DCB specimen, the restrictive condition of specimen dimensions which allows the crack to grow at the interface is mitigated. A similar discussion is valid for a MMB specimen. The crack is susceptible to steady-state interfacial growth in a sandwich specimen with residual thermal stresses compared to one without residual thermal stresses.

5. Concluding remarks

In the present study, the necessary geometric condition was derived for interfacial debond characterization of foam core sandwich beams. The recommended specimen geometry (i.e. thickness) was presented.

The first part of the paper summarized the crack kinking analysis of foam core sandwich beam. It was demonstrated that steady-state crack position in foam core sandwich specimens for fracture characterization can be predicted based on the comparison to experimental data.

Then, the condition for steady-state crack growth along the interface between the face sheet and the core was derived for the cases of several test methods (i.e. DCB, SCB, and MMB tests). Geometric condition of the specimen that enables the interfacial debond charac-

terization (i.e. face sheet thickness/core thickness) was shown in the graphic form and the approximated equation.

Finally, it was shown that the derived condition is equivalent to the strain difference between the upper and lower crack surfaces. The effect of residual thermal stresses on the necessary condition was also explained. In the case of typical foam core sandwich specimens, it was concluded that the restrictive condition of specimen dimensions which allows the crack to grow at the interface is mitigated.

The present paper gives fundamental knowledge on the specimen geometry of foam core sandwich specimen for debond characterization. Specimen geometry (thickness ratio) can be designed a priori using the derived figure and equation. The present results will contribute to the efficient development of light-weight foam core sandwich structures, the feasibility study of foam core sandwich structures, and the standardization of testing method for fracture characterization of foam core sandwich specimens.

Acknowledgment

The author gratefully acknowledges the support of Mizuho Foundation for the Promotion of Sciences.

References

[1] Herrmann A, Zahlen PC, Zuardy I. Sandwich structures technology in commercial aviation, *Proceedings of the 7th International Conference on Sandwich Structures*. Denmark: Aalborg; 2006. 13–26.
[2] Nokkentved A, Lundsgaard-larsen C, Berggreen C. Non-uniform compressive strength of debonded sandwich panels – I. Experimental investigation. J. Sandwich Struct. Mater. 2005;7:461–482.
[3] Berggreen C, Simonsen BC. Non-uniform compressive strength of debonded sandwich panels – II. Fracture mechanics investigation. J. Sandwich Struct. Mater. 2005;7:483–517.
[4] Shipsha A, Burman M, Zenkert D. Interfacial fatigue crack growth in foam core sandwich structures. Fatigue Fract. Eng. Mater. 1999;22:123–131.
[5] Grenestedt JL. Development of a new peel-stopper for sandwich structures. Compos. Sci. Technol. 2001;61:1555–1559.
[6] Jakobsen J, Bozhevolnaya E, Thomsen OT. New peel stopper concept for sandwich structures. Compos. Sci. Technol. 2007;67:3378–3385.
[7] Hirose Y, Matsuda H, Matsubara G, Inamura F, Hojo M. Evaluation of new crack suppression method for foam core sandwich panel via fracture toughness tests and analyses under mode-I type loading. J. Sandwich Struct. Mater. 2009;11:451–470.
[8] Aviles F, Carlsson LA. Analysis of the sandwich DCB specimen for debond characterization. Eng. Fract. Mech. 2008;75:153–168.
[9] Carlsson LA, Matteson RC, Aviles F, Loup DC. Crack path in foam cored DCB sandwich fracture specimens. Compos. Sci. Technol. 2005;65:2612–2621.
[10] Ratcliffe JG. Sizing single cantilever beam specimens for characterizing facesheet/core peel debonding in sandwich structure. NASA-TP 2010-216169. 2010.
[11] Ratcliffe JG, Reeder JR. Sizing a single cantilever beam specimen for characterizing facesheet–core debonding in sandwich structure. J. Compos. Mater. 2011;45:2669–2684.
[12] Li X, Carlsson LA. The tilted sandwich debond (TSD) specimen for face/core interface fracture characterization. J. Sandwich Struct. Mater. 1999;1:60–75.
[13] Li X, Carlsson LA. Elastic foundation analysis of tilted sandwich debond (TSD) specimen. J. Sandwich Struct. Mater. 2000;2:3–32.
[14] Quispitua A, Berggreen C, Carlsson LA. On the analysis of a mixed mode bending sandwich specimen for debond fracture characterization. Eng. Fract. Mech. 2009;76:594–613.
[15] Yokozeki T. Analytical study on the fracture toughness characterization tests of foam core sandwich specimens. J. Jpn. Soc. Aeronaut. Space Sci. 2011;59:16–24. Japanese.
[16] Yokozeki T. Analysis of crack kinking in foam core sandwich beams. Compos. Part A. 2011;42:1493–1499.
[17] Erdogan F, Sih GC. On the crack extension in plates under plane loading and transverse shear. J. Basic Eng. 1963;85:519–527.